Pergamon

Geochimica et Cosmochimica Acta, Vol. 64, No. 12, pp. 2119–2132, 2000

0016-7037/00 $20.00 + .00

PII S0016-7037(00)00358-6

Helium isotope ratios in mafic phenocrysts and geothermal fluids from La Palma, the Canary Islands (Spain): Implications for HIMU mantle sources

D. R. HILTON[a,*] C. G. MACPHERSON,[a,†] and T. R. ELLIOTT[b,‡]

[a] Geosciences Research Division, Scripps Institution of Oceanography, University of California, San Diego, La Jolla, CA 92093-0244, USA
[b] Department of Earth Sciences, Vrije Universiteit, De Boelelaan 1085, 1081 HV Amsterdam, The Netherlands

(*Received March* 29, 1999; *accepted in revised form January* 20, 2000)

Abstract—We report a comprehensive study of He isotope ($^3He/^4He$) variations on well-characterized lavas from La Palma, the current locus of activity of the Canary hotspot. Cogenetic olivine (OL) and clinopyroxene (CPX) phenocrysts from 11 basaltic lava flows representing all stages of the island's evolution were analyzed by crushing in vacuo. Additionally, the sample set is supplemented by a CO_2-rich bubbling cold spring in Taburiente caldera. Phenocryst $^3He/^4He$ ratios vary between 6.3 to 8.9R_A; both extremes occur in the 2 to 0.6 Ma shield-building Taburiente lavas. Historic flows vary between 7.0 to 7.8R_A, whereas phenocrysts from a single submarine basement sill (4.0–2.9 Ma) have $^3He/^4He$ ratios of 8.3R_A (OL) and 8.4R_A (CPX). He isotopic equilibrium characterizes all the phenocryst pairs except one Taburiente lava. The absence of a correlation between $^3He/^4He$ and [He] contrasts with other ocean island basalts, e.g., Heard Island (Hilton et al., 1995) and, together with equilibrium in phenocrystic $^3He/^4He$, suggests that the La Palma sample suite has $^3He/^4He$ ratios that have suffered minimal crustal contamination. The cold spring (geothermal) sample gives a $^3He/^4He$ ratio of 9.5R_A, which is higher than any of the phenocrysts and in excellent agreement with a previously reported value for Taburiente caldera (Perez et al., 1996). The geothermal $^3He/^4He$ values indicate that La Palma is the first HIMU-like ocean island (where HIMU implies a distinctive mantle source with high time-integrated $^{238}U/^{204}Pb$ (μ) ratio) with reported $^3He/^4He$ ratios higher than the canonical value (8 ± 1R_A) characteristic of depleted mid-ocean ridge basalt (MORB) mantle.

We present two simple mixing scenarios that are compatible with the He–Pb isotope systematics of La Palma: a) a high-^3He mantle plume, extensively but variably depleted in its original He content, mixes with a HIMU source characterized by both radiogenic He and lead isotope compositions; and b) mixing between a composite plume, with high $^3He/^4He$ and radiogenic lead, and depleted mid-ocean ridge basalt mantle. The latter model is favored as it appears to account more readily for the mid-ocean ridge MORB-like He isotope characteristics of the lavas. Addition of radiogenic He—most likely produced in mantle melts frozen into the sub-Canarian mantle lithosphere—to resultant mixtures may subsequently occur in either model. Such a process can explain the absence of correlations between He and Pb isotope ratios in the lavas, and the lower $^3He/^4He$ values of the phenocrysts with respect to the geothermal fluids. We find no need to invoke a radiogenic growth/diffusion model (Hanyu and Kaneoka, 1998) to explain the He–Pb isotope relationships for La Palma. These mixing models may also be applicable to other HIMU islands: however, any high-^3He plume signature of St. Helena and Mangaia may be obscured due to the high proportion of the HIMU component at these localities and/or by addition of radiogenic He.

1. INTRODUCTION

He isotope ($^3He/^4He$) ratios in ocean island basalts (OIB) are highly variable, from ratios as high as ~30 to 38R_A (where R_A = air $^3He/^4He$) at Hawaii and Iceland to values as low as ~5 to 7R_A at St. Helena, Tubuaii, and Mangaia. The data set is bimodal and straddles the near constant $^3He/^4He$ ratios of 8 ± 1R_A found in midocean-ridge basalts (MORB) worldwide (see Farley and Neroda, 1998 and references therein for a recent summary of OIB and MORB $^3He/^4He$ ratios, plus Hilton et al., 1999 for a report of the highest values worldwide). Interpretation of these variations in OIB He isotope ratios invariably call for distinct mantle reservoirs with the highest values ('high-^3He' hotspot ratios) thought to represent plume material originating within the lower mantle (Craig and Lupton, 1976) or at the core–mantle boundary (Macpherson et al., 1998), and lower values (<MORB: so-called 'low-^3He' hotspot ratios) that are argued to contain one or more recycled components, possibly entrained in or upwelling as mantle plumes (Graham et al., 1992; Hanyu and Kaneoka, 1997; Kurz et al., 1982a).

More detailed discussion on the significance of the variability of $^3He/^4He$ ratios in OIB (e.g., Farley and Craig, 1992; Graham et al., 1993; Graham et al., 1992; Hart et al., 1992b) has centred upon the 'mantle tetrahedron' of Hart et al. (1992a) in which all the radiogenic isotope data of OIB (and MORB) are enclosed within a tetrahedron whose apices are defined by extrema in the radiogenic isotope data. A crucial observation is that the 'low-^3He hotspots' are found towards the apices of the tetrahedron: at HIMU islands Mangaia, St. Helena, and Tubuaii and EM II island Tristan da Cunha (Graham et al., 1992; Hanyu and Kaneoka, 1997; Kurz et al., 1982a). The association of $^3He/^4He$ ratios < MORB with extreme Sr–Nd–Pb isotopic compositions has been commented upon as "consistent with a

* Author to whom correspondence should be addressed (drhilton@ucsd.edu).
† *Present address*: Department of Geology, Royal Holloway University of London, Egham, Surrey, TW20 0EX, UK (E-mail: c.macpherson@gl.rhbnc.ac.uk).
‡ *Present address*: Department of Geology, University of Bristol, Queens Road, Bristol, BS7 1RJ UK (Tim.Elliott@bristol.ac.uk).

recycled origin" (Graham et al., 1993; Graham et al., 1992), yet the actual range of $^3He/^4He$ ratios measured (5–8R_A) is significantly greater than the radiogenic values [~0.05R_A; (Morrison and Pine, 1955)] anticipated for ancient recycled material. To explain this apparent discrepancy, a model involving diffusive exchange of He between ancient recycled material and ambient MORB mantle has been developed (Hanyu and Kaneoka, 1998).

An alterative explanation proposed to account for OIB $^3He/^4He$ ratios < MORB (the 'low-^{3}He' hotspots) is the possibility that some OIB lavas could be contaminated with crustal (radiogenic) He as a consequence of gas loss and assimilation in near-surface magma chambers. The observation (Hilton et al., 1995) that the category of 'low-^{3}He' hotspots was defined mainly by He-poor phenocryst samples, especially clinopyroxenes (CPXs), led to the suggestion that the initial $^3He/^4He$ ratios of isotopically extreme OIBs could have been higher and that all four apices of the mantle tetrahedron may have been characterized by $^3He/^4He$ ratios of at least 8 R_A. Accounting for the origin of the radiogenic He component in isotopically extreme OIBs (such as HIMU islands) is problematic, therefore, but remains an important goal with implications for the origin of deep-seated plumes, their mixing histories in the mantle and/or the means by which they interact with the lithosphere before eruption.

In this contribution, we utilize both phenocryst-bearing lavas and present-day geothermal emissions to report a detailed He isotope study of an ocean island (La Palma in the Canary Islands) exhibiting characteristic HIMU-like geochemical traits. A key consideration in choosing La Palma, as opposed to the classic HIMU islands with more radiogenic lead isotope ratios, is that La Palma is the active manifestation of the Canary Islands hotspot with a well-constrained eruption history (e.g., Ancochea et al., 1994; Staudigel et al., 1986). There is abundant fresh material, all of sufficient youth that there is no need to consider posteruptive effects on $^3He/^4He$ ratios that may have possibly influenced data from other (older) HIMU localities. By examining for He isotopic equilibrium between phenocryst pairs in lavas with well-documented (HIMU-like) trace element, lead isotope and, particularly, osmium isotope characteristics (Elliott, 1991; Marcantonio et al., 1995), we obtain important independent constraints on how $^3He/^4He$ ratios may have been affected en route to the surface. We argue that La Palma is the first HIMU-like ocean island with reported high-^{3}He hotspot characteristics (≥9.6 R_A), and we show that the range of observed $^3He/^4He$ ratios is consistent with simple mantle mixing models that, additionally, involve the superimposition of radiogenic He most likely from the sub-island mantle lithosphere. We find no need to invoke a radiogenic growth–diffusion model (e.g., Hanyu and Kaneoka, 1998) for La Palma, and suggest that plume degassing, mantle mixing, and addition of radiogenic He are the principal factors controlling the He isotope characteristics of this and possibly other HIMU ocean islands.

2. GEOLOGICAL BACKGROUND AND SAMPLES

La Palma is situated at the northwestern extreme of the ~500 km Canary Islands hotspot chain off the NW coast of Africa (Fig. 1). The island is built on oceanic crust of Jurassic age (155 Ma) (Hayes and Rabinowitz, 1975) and rises ~6500 m above the surrounding sea-floor exposing a ~1800 m thick sequence of submarine and subaerial volcanics (Staudigel and Schmincke, 1984). A conspicuous feature of the island is the Caldera de Taburiente, the eroded remnant of a depression suggested to have formed by lateral collapse of an earlier volcanic edifice (Ancochea et al., 1994; Gillou et al., 1998), which valuably exposes the submarine stratigraphy of the island.

The geology of the island can be separated into two distinct units: the older Seamount Series (4–2.9 Ma) and a younger subaerial complex known as the Coberta Series. The Seamount Series can be divided into three parts: 1) submarine basaltic and trachytic lavas; 2) a dense swarm of mostly basaltic sills and dikes; and 3) gabbroic intrusions (Staudigel and Schmincke, 1984). It outcrops at the bottom of the Caldera de Taburiente in the Barranco de las Angustias (Fig. 1). The Coberta Series covers most of the island and consists of the older Taburiente Series (2–0.6 Ma), that forms the major shield volcano at the north of the island, and younger (0.6–0 Ma) lavas that have produced the southern Cumbre Vieja ridge (Ancochea et al., 1994; Gillou et al., 1998). The latter has been likened to a Hawaiian-style rift zone (Ancochea et al., 1994). The older Coberta Series is well-exposed in the caldera walls of the older northern part of the island, whereas historic lavas are associated with the Cumbre Vieja volcanic ridge which occupies the south of the island.

Lavas of La Palma are highly alkalic basalts and basanites, with distinctive trace element and isotopic signatures (Elliott, 1991; Marcantonio et al., 1995; Widom et al., 1999). Lead isotope ratios are notably radiogenic, with $^{206}Pb/^{204}Pb$ ranging from 19.2 to 20. Although these values fall short of the extreme values found on the HIMU islands of St. Helena, Tubuaii, and Mangaia, the La Palma lavas additionally share a set of characteristic chemical signatures as extreme as lavas from these classic HIMU localities (cf. Weaver, 1991). In particular, La Palma lavas show very low La/Nb (mean 0.76 for the samples of this study) and some of the most radiogenic (magmatic) $^{187}Os/^{188}Os$ found in ocean islands basalts (Marcantonio et al., 1995; Widom et al., 1999). As noted by Marcantonio et al. (1995), the combined chemical evidence strongly suggests that La Palma lavas sample a source that has experienced processes essential to the production of HIMU mantle, even if fractionation of U/Pb, the key labeling index, is not quite as marked as the classic localities.

The majority of samples analysed in the present work represent the Coberta Series: five from the main Tuburiente Shield building phase (2–0.6 Ma) and five historic flows. A single mafic sill (93LP134) from the Basement Complex was also analyzed. The subaerial Coberta lavas are generally very fresh, showing little indication of posteruptive alteration, and contain up to 40% (OL), CPX, and titanomagnetite phenocrysts. Petrographic descriptions, major and minor element geochemistry, Sr, Nd, Pb isotope ratios and, in most cases, Os isotope data are available on the sample suite (Elliott, 1991; Marcantonio et al., 1995). The geothermal fluid is a present-day (sampled in 1996) CO_2-rich bubbling cold spring situated within the Tuburiente caldera (Fig. 1).

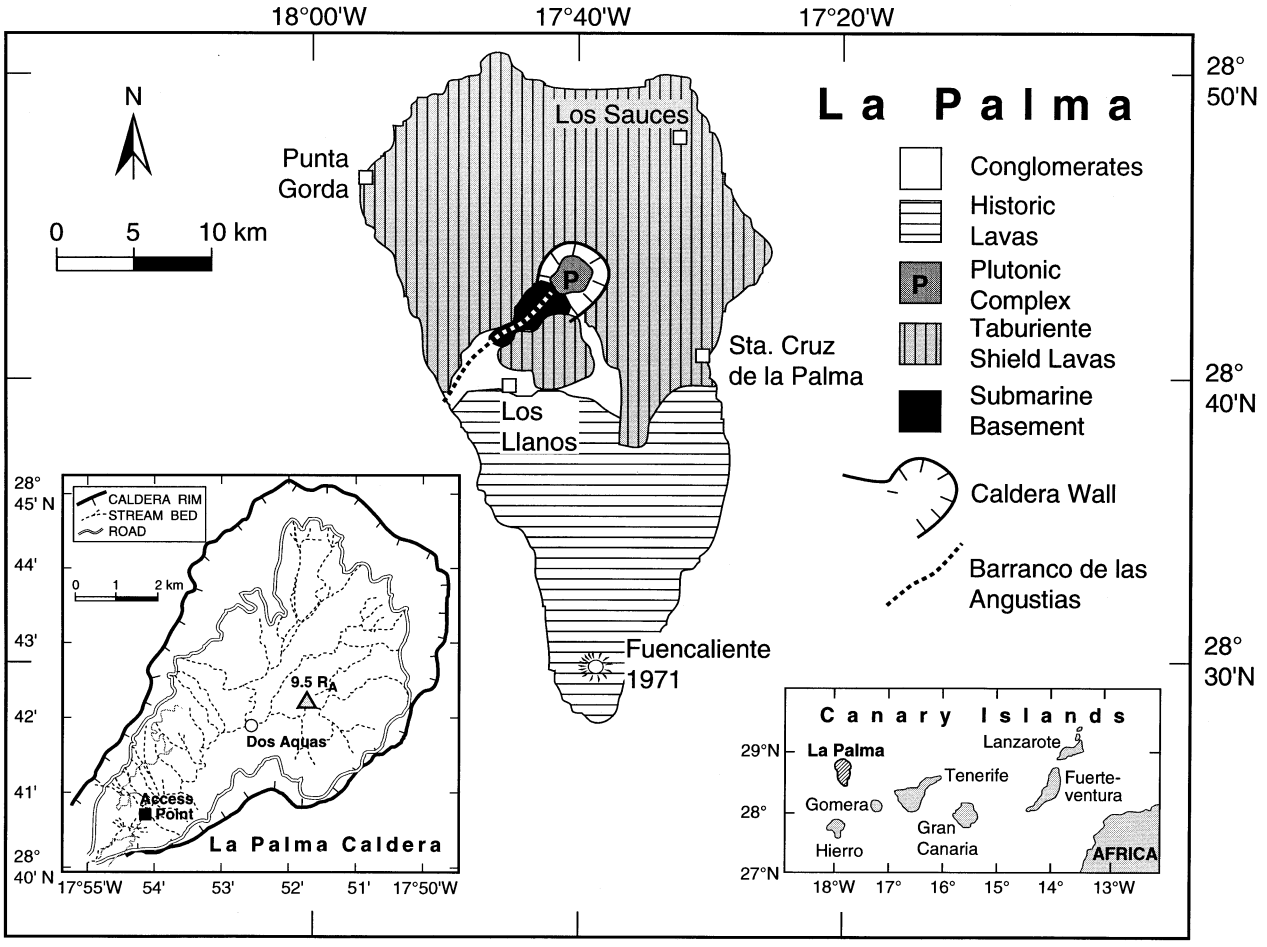

Fig. 1. Simplified geological map of La Palma, The Canary Islands (modified from Marcantonio et al., 1995) showing the Cumbre Vieja, site of all historic eruptions, in the south of the island and the Taburiente Shield series in the north. The Basement Complex outcrops in the Barranco de las Angustias. Inset left shows the location of the geothermal fluid (this work) in relation to that sampled by Perez (Perez et al., 1996) at Dos Aguas; inset right is the location of the Canary Islands off the northwest coast of Africa.

3. ANALYTICAL METHODS

All phenocryst samples were hand-picked from crushed whole rocks with the aid of a binocular microscope. Mineral separates were then cleaned using an acetone/methanol mixture and dried at 110°C before a final picking stage, carried out to ensure that all separates were free of adhering matrix material.

Phenocrysts were loaded into on-line crushers (three were connected to the preparation line) and pumped to ultra-high vacuum (UHV) overnight. After analysis of the Isotope Laboratory MM (Murdering Mudpots, Yellowstone) standard (16.45 $R_A \pm 4.5\%$; 2σ, $n = 16$), a crusher blank was carried out for a 4-min period. The crushers employ a hardened-steel slug raised and lowered by an external magnet. When sufficiently low blanks were achieved, typically <0.5 ncm^{3}STP^{4}He, the sample was released (without breaking vacuum) into the crusher past slots in the slug and a 4-min crush was initiated. Released volatiles were exposed sequentially to hot titanium, a charcoal finger held at -196°C and a He-cooled cryogenic trap designed to isolate He from neon. He was then expanded into a split-tube rare gas mass spectrometer (GAD) with a Faraday cup for ^{4}He measurement and an electron multiplier for detecting ^{3}He (Rison and Craig, 1983). The system blank constituted less than 7% of the total gas in all samples except LP95b-ol (9.7%), 96LP-cpx (13.1%), 93LP110-cpx (15.5%), 93LP113-cpx (15.6%), 93LP106-ol (18.0%), 93LP107-ol (18.0%), 93LP106-cpx (41.3%), and LP43e-ol (41.2%). Following sample analysis, an aliquot of the MM standard, similar in ^{4}He abundance to the sample, was prepared, analyzed and used to normalize the blank-corrected ^{3}He/^{4}He ratio. Reproducibility in [He] of the MM standard at aliquot sizes 1 to 20 ncm^{3}STP was $\pm 6.5\%$ (2σ) over the course of this work.

The geothermal sample was collected in an evacuated 1720-glass flask and extracted by using a dedicated 1720-glass line equipped with in-line Hg diffusion and toepler pumps. An aliquot of the noncondensable gas was collected in a breakseal for transfer to GAD for He isotope analysis. CO_2 content was measured manometrically. Further details are given in Hilton (1996).

4. RESULTS

4.1. He Isotope Ratios

He isotope and concentration results of 11 cogenetic OL and CPX phenocryst pairs (representing samples from the Basement Complex, and the older and younger Coberta Series) together with that of the geothermal fluid from within Tuburiente caldera are reported in Table 1. The highest ^{3}He/^{4}He ratio of the present study (reported in the R/R_A notation, where R = sample ^{3}He/^{4}He and R_A = air ^{3}He/^{4}He) is found for the geothermal fluid sample (9.50 R_A) and confirms reports of high

Table 1. Phenocryst and geothermal fluid He isotope and abundance results and whole-rock lead abundance and $^{206}Pb/^{204}Pb$ isotope results.

Sample	Phase	Weight (mg)	[He] ncm^3 STP/g	R/R_A ($\pm 2\sigma$)	$\frac{^{206}Pb}{^{204}Pb}$	[Pb] (ppm)
Historic flows						
LP30e	OL	460	37.0	7.38 ± 0.35	n.d.[a]	n.d.
	CPX	420	48.7	7.19 ± 0.34		
71LP41	OL	460	45.6	7.57 ± 0.33	19.575	2.92
	CPX	600	83.5	7.37 ± 0.25		
LP43e	OL	100	23.2	7.49 ± 0.96	19.611	n.d.
	CPX	530	56.0	7.33 ± 0.27		
151LP69e	OL	790	30.2	7.82 ± 0.21	19.579	3.21
	CPX	850	57.3	7.63 ± 0.22		
LP95b	OL	400	49.7	7.04 ± 0.27	19.668	n.d.
	CPX	540	37.2	7.28 ± 0.33		
Main Taburiente Shield (1.6–0.8 Ma)						
96LP46	OL	900	16.5	8.04 ± 0.34	n.d.	n.d.
	CPX	810	8.5	7.72 ± 0.49		
93LP106	OL	900	2.7	8.92 ± 0.69	19.938	1.95
	CPX	850	0.7	7.94 ± 4.72		
93LP107	OL	910	2.2	7.10 ± 1.48	20.010	1.30
	CPX	920	4.2	7.35 ± 0.79		
93LP110	OL	870	11.6	6.77 ± 0.46	19.812	2.15
	CPX	500	3.1	7.24 ± 1.48		
93LP113	OL	850	11.3	8.00 ± 0.29	19.877	2.51
	CPX	860	3.0	6.35 ± 1.02		
Basement complex (4.0–2.9 Ma)						
93LP134	OL	900	44.7	8.30 ± 0.23	19.942	2.03
	CPX	900	28.6	8.41 ± 0.27		
Geothermal fluid (Taburiente Caldera)						
96LP1	CO_2-spring		1.7×10^{10}[b]	9.50 ± 0.27		

[a] n.d. = not determined.
[b] $CO_2/^3He$ ratio.

fluid $^3He/^4He$ ratios ($^3He/^4He = 9.68\ R_A$; Perez et al., 1996) in the caldera (see Fig. 1). These two fluid values appear significantly greater than the nominal MORB ratio of $8 \pm 1\ R_A$ (Farley and Neroda, 1998), and would seem to indicate that La Palma is sampling He of the 'high-^{3}He' hotspot variety ($^3He/^4He >$ MORB values) as found in geothermal fluids on other ocean islands such as Hawaii and Iceland (see recent reports in (Hilton et al., 1998a; Hilton et al., 1997). The integrity of these two geothermal fluid $^3He/^4He$ ratios as diagnostic of the La Palma magmatic system, and the significance of the absolute values as indicators of mantle plume involvement are discussed in detail in Section 5.

The highest phenocryst $^3He/^4He$ ratio (8.92 R_A) is found in OLs from the main Taburiente Shield lavas but this series also shows the lowest value (6.35 R_A) of the present study. Although the highest ratio appears at the upper end of the MORB range, the average ratio of the series, $7.54 \pm 0.73\ R_A$ ($n = 10$, 1σ), is slightly lower than the MORB average but is overlapping within error. The historic lavas range from 7.04 to 7.82 R_A, have a slightly lower mean value ($7.40 \pm 0.23\ R_A$; $n = 10$) but again overlap the MORB range. Cogenetic phenocrysts from the single Basement Complex sample have slightly higher $^3He/^4He$ ratios of 8.30 R_A (OL) and 8.41 R_A (CPX)—both values well within error of the MORB ratio. These values agree within error with a ratio of 8.7 R_A reported for a picrite from the Pliocene series of Taburiente Caldera (Graham et al., 1996).

Significantly, there appears little correspondence or coupling between He and lead isotopes for the present sample suite (Table 1). For example, sample 93LP107 has the most radiogenic $^{206}Pb/^{204}Pb$ ratio (20.01) yet both LP95b (7.28 R_A) and 93LP110 (7.24 R_A) have lower $^3He/^4He$ values. Similarly, sample 93LP106 (8.9 R_A) has the highest phenocryst $^3He/^4He$ ratio, yet its $^{206}Pb/^{204}Pb$ (19.94) ratio is one of the most radiogenic of the samples analysed. This is a surprising result given the general notion that ancient recycled material should produce both radiogenic He and lead. In Section 5.4, we consider possible explanations for this observation.

4.2. He Isotope Variations Between Co-genetic Mineral Pairs

When the He isotope systematics of mineral pairs of the same sample are considered (Fig. 2) a remarkable feature of the La Palma dataset is that the majority (10 out of 11 sample pairs) display He isotope equilibrium between cogenetic OL and CPX phenocrysts. Equilibrium in $^3He/^4He$ ratio (i.e., within analytical error samples plot coincident with the equiline in Fig. 2) occurs irrespective of lava series and over a wide range of He concentrations (from <1 to 84 ncm^{3}STP/g; Fig. 3): only one sample (93LP113 from the Taburiente Shield) does not show this equilibrium, and it has a distinctly higher $^3He/^4He$ ratio in the OL (8.0 R_A) compared to the CPX (6.35 R_A). With the exception of this one sample, the observation of $^3He/^4He$ equilibrium between phenocryst pairs in the other Taburiente series lavas argues strongly against modification of the measured $^3He/^4He$ ratios since crystallization of these mineral phases (Hilton et al., 1995; Hilton et al., 1993b; Marty et al., 1994; see Section 5.1).

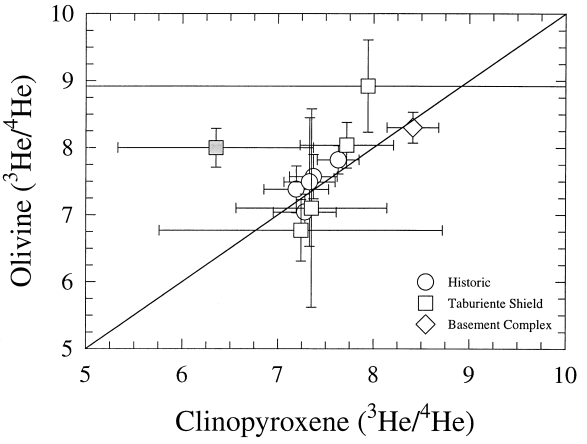

Fig. 2. He isotope ratios (R/R_a notation) in cogenetic OL and CPX phenocrysts for La Palma lavas (Table 1). The solid diagonal line (equiline) represents He isotope equilibrium between the two mineral phases. All samples in the present study fall on the equiline (within 2σ analytical error) except for sample 93LP113 (shaded).

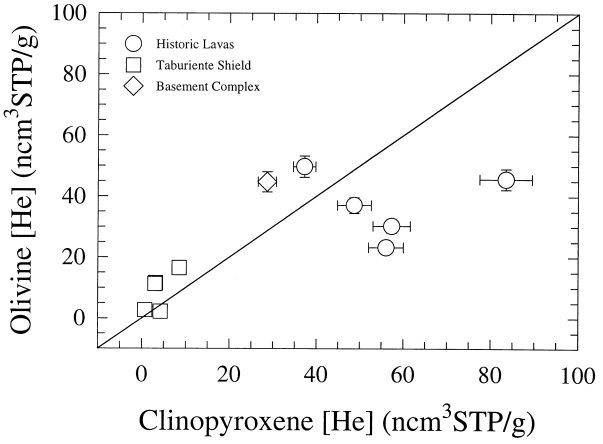

Fig. 4. Comparison between observed He concentrations in OL vs. CPX phenocrysts for La Palma samples (Table 1). The solid diagonal line (equiline) represents equal concentrations in the two phenocryst phases. Note that in four of five cases, He concentrations are greater in the OLs for the Taburiente Shield lavas whilst the opposite is the case for the Historic flows. The single Basement Complex lava follows the pattern of the majority of the Historic phenocrysts.

4.3. He Abundance Characteristics of Phenocryst Phases

Despite the overlap in He isotope ratios, the He concentrations [He] in the phenocryst phases vary significantly between the three lava series (Fig. 4). Although no samples have the same [He] in OL and CPX pairs, the historic lavas have consistently high [He] (between 23 and 84 ncm^{3}STP/g) with higher concentrations in the CPXs than cogenetic OLs in four of five cases (i.e., most samples lie below the equiline in Fig. 4). All the Taburiente Shield phenocrysts have significantly lower [He] (between 0.7 and 17 ncm^{3}STP/g) with cogenetic OLs having the greater concentrations in 4 out of 5 cases. Within error, the single Basement Complex sample (93LP134) has the second highest OL [He] (44.7 ncm^{3}STP/g) of the present study but a significantly lower CPX [He] displacing it away from the historic lavas in Figure 4. Similar variability in [He] between different lava series have been reported for the Juan–Fernandez archipelago (Farley et al., 1993) and ascribed to variations in He abundances in the source mantle. We suggest that the apparent temporal control on the [He] for La Palma phenocrysts may also reflect differences in volatile degassing behaviour between the more active main shield-building phase and present-day rift volcanism.

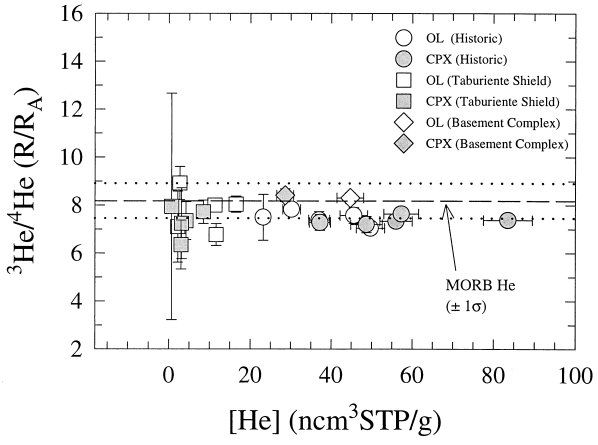

Fig. 3. Plot of He isotope ratios (^{3}He/^{4}He) vs. He concentrations for all phenocrysts in this study (from Table 1). Open symbols represent OL phenocrysts and closed symbols represent CPXs. The average MORB ^{3}He/^{4}He ratio ($8.18 \pm 0.73R_A$) is taken from Hilton et al., (1993a). Note that all phenocryst samples, irrespective of volcanic series, plot coincident with the MORB ^{3}He/^{4}He ratio (within 1σ error) except two low [He] samples: 93LP110-OL ($6.77R_A$) an 93LP113-CPX ($6.35R_A$).

5. DISCUSSION

Before considering the implications of the He isotope results at La Palma for the nature and development of a HIMU-like mantle endmember, we consider first the integrity of the He isotope results in an attempt to avoid ascribing features potentially related to the entrapment, storage and/or transport of the He to mantle sources supplying La Palma. This allows for a more rigorous assessment of the source affinity of the He—both in the case of geothermal fluids and phenocrysts—as being MORB source or plume mantle with the concomitant implications for the nature and development of those sources.

5.1. Magma Ageing, Crustal Contamination, and Tritium Decay

The wide range in La Palma ^{3}He/^{4}He ratios (6.8–9.6 R_A) derived from both geothermal fluids (Perez et al., 1996 and this work) and phenocryst-bearing lavas (Graham et al., 1996 and this work) raises the possibility that one or both sampling media may have modified the He isotopic signature characteristic of the underlying (mantle) source. For example, if the geothermal fluids contained significant tritium then subsequent decay to ^{3}He would result in an increase in the ^{3}He/^{4}He ratio, possibly shifting a MORB-type value into the lower range of high-^{3}He hotspot He. Alternatively, some of the phenocrysts ratios could have low ^{3}He/^{4}He values as a consequence of

preeruptive magma chamber ageing and/or upper crustal contamination—the effects of which would be exacerbated by degassing via near-surface magma chambers. For the historic lavas, at least, posteruptive modification of the $^3He/^4He$ ratios can be ruled out by young eruption ages. Similarly, preservation of mineral pair He isotopic equilibrium in the Basement Complex and Taburiente series lavas effectively excludes this process for these samples also (see Section 4.2). If none of the aforementioned processes have compromised the measured $^3He/^4He$ values then variations in the $^3He/^4He$ signature—recorded here for the ~4 Ma volcanic history of La Palma—must have occurred either in the underlying mantle lithosphere or mantle source region.

The possibility that residence of magma in the crust (magma ageing: (Zindler and Hart, 1986) could account for the difference between the fluid (9.6 R_A) and phenocryst $^3He/^4He$ ratios (7.61 $\pm$ 0.52 R_A; $n = 21$, excluding the value of 6.35 R_A) can be evaluated with reference to two endmember scenarios. In the first (closed system) case, we assume that magma contains He with $R/R_A = 9.6$ at a concentration equivalent to MORB source ($\sim 15 \times 10^{-6}$ cm^3STP/g; see Appendix). Given the expectation that hotspot sources are likely to contain higher He contents (Porcelli and Wasserburg, 1995), the adopted value thus represents a minimum estimate. For a uranium content of 1.6 ppm and Th/U = 3.8 (Elliott, 1991), a crustal residence time of ~10 Myr would be necessary to grow in the requisite radiogenic He to produce the change in $^3He/^4He$. Such a period is wholly implausible given observations of U-series disequilibrium on the present sample suite (Elliott, 1991), and estimates of magma ascent rates (<100 h) and residence times of magma in crustal reservoirs (decades) at La Palma based upon xenolith eruption mechanics and fluid inclusion barometry respectively (Klugel, 1998; Klugel et al., 1997). Indeed, initial He concentrations in the magma source would have to be an unprecedented 5 orders of magma lower than that envisaged for MORB source if closed-system ageing were to affect magma $^3He/^4He$ ratios over timescales of hundreds of years. Alternatively, in the second (open) system case, the original magma would have to have been degassed of its mantle-derived He to ~0.001% of its original concentration before residence in the crust for characteristic time scales of 100s of years to grow in sufficient ^4He to decrease the $^3He/^4He$ ratio by the requisite amount. In either case, the concentration of He in the magma ($\sim 1 \times 10^{-10}$ cm^3STP/g with a ratio of 7.61 R_A) would give equilibrium OL and CPX He contents $\sim 1 \times 10^{-14}$ cm^3STP/g (see review in Carroll and Draper, 1994). This value is approximately 5 orders of magnitude lower than measured values so that the modified magma He would have a negligible effect on He trapped in phenocrysts. We conclude that magma ageing in the crust has had an insignificant effect on initial $^3He/^4He$ ratios.

The extent to which crustal contamination has modified measured $^3He/^4He$ ratios can be addressed through a comparison of measured values in cogenetic OL and CPX phenocrysts (Hilton et al., 1995). Because the diffusivity of He in CPX at magmatic temperatures is approximately an order of magnitude greater than in OL (Trull and Kurz, 1993), CPXs are likely to preferentially sample any crustal (radiogenic) He incorporated into magma en route to the surface (Hilton et al., 1995; Hilton et al., 1993b; Marty et al., 1994). The observation of isotopic equilibrium for the La Palma phenocryst pairs, therefore, indicates that crustal He contamination was absent at La Palma or magmatic He was trapped at sufficiently high concentration at depth, by crystallization during magma stagnation in the mantle for example, to completely negate any crustal input. The trapping of He at mantle depths is fully consistent with observations of: a) high-density fluid inclusions in OL phenocrysts, e.g., from the 1949 eruption (Hansteen et al., 1998); and b) nearly all samples (this study) lack plagioclase phenocrysts (Elliott, 1991), which indicates crystallization pressures in transitional alkalic lavas greater than 5 to 8 kbar (15–24 km depth) (Fisk et al., 1988). The OLs themselves would be insulated from the possibility of late-stage He re-equilibration at shallower levels due to their lower He diffusivity and lack of cleavage. The observation of He isotopic equilibrium in these particular samples, therefore, argues against modification of $^3He/^4He$ due to addition of radiogenic He following crystallization of the phenocrysts, and therefore excludes a crustal source of radiogenic He as the cause of the variations in $^3He/^4He$ ratios.

The effect of tritium decay on the geothermal fluids is more difficult to assess, as no direct measurements are available: however, significant limiting constraints can be placed on its possible influence. The closest precipitation monitoring station to the Canary Islands is Gibraltar where tritium contents reached a maximum value of 504 TU (where 1 TU = 1 tritium atom in 10^{18} H atoms) in 1963 following the moratorium on atmospheric thermonuclear device testing the previous winter (IAEA, 1992). For thermonuclear tritium to modify MORB-like $^3He/^4He$ ratios (8 ± 1 R_A; see Section 5.2) to values of 9.6 R_A, then: 1) the 1996 geothermal fluids would have to contain a substantial fraction of the 1963 precipitation; 2) the geothermal system must have remained closed to gas loss since recharge; and 3) bubble formation must have occurred immediately before sampling. Because direct measurements are unavailable for La Palma it is difficult to refute this possibility conclusively, but we believe it *extremely unlikely* that any of the measured ^3He in the fluids originates from recent, tritiated water. In addition to the unlikely possibility that the fluids meet the previous three conditions, the following considerations also argue against a contribution from bomb tritium: a) the two geothermal localities in the Taburiente caldera (see Fig. 1 inset) have overlapping (within error) $^3He/^4He$ ratios: this would require that outflow localities over 1 km apart would have to fortuitously sample fluids of exactly the same age or with exactly the same proportion of tritiated water; b) mass balance considerations at other localities, e.g., Iceland (see Hilton et al., 1990 and Poreda et al., 1992), with documented high tritium contents in postbomb precipitation (~1200 TU; (Theodorsson, 1967) have failed to identify any contribution of tritiogenic ^3He to geothermal fluid ^3He inventories; and c) the measured $CO_2/^3He$ of 1.7×10^{10} (Table 1) is already high compared with the range observed in MORB and hotspots (Hilton et al., 1998b; Hilton et al., 1997; Marty and Jambon, 1987; Trull et al., 1993). The presence of a tritiogenic-^3He component would mean that the ratio would have to have been even higher and further displaced from a characteristic 'magmatic' value.

We conclude, therefore, that both the mafic phenocrysts and geothermal fluids sample He that is essentially unmodified in

isotopic composition after crystallization of the phenocryst phases and/or during transport by the geothermal system through the crust.

5.2. Provenance of La Palma Helium: Plume or MORB Mantle?

The combined He isotope database for La Palma (6.8–9.6 R_A; this work and Graham et al., 1996; Perez et al., 1996; Vance et al., 1989) straddles the range nominally associated with MORB mantle (8 ± 1 R_A). The geothermal fluid values pose a problem in that they fall either at the uppermost extreme of the MORB range or at the lowermost boundary of 'high-^{3}He' hotspot range. In attempting to assign a MORB or plume source provenance to the He sampled by the geothermal fluids, therefore, it is vital to determine the uppermost defining limit of MORB-He. Comparing the fluid values to this limit has clear ramifications for understanding both the He isotope systematics of HIMU mantle and the role of mantle plumes in the petrogenesis of La Palma (Section 5.4).

The canonical MORB ^{3}He/^{4}He ratio of 8 ± 1 R_A referred to above is derived from a number of compilations of He isotope data. In chronological order, the following values have been reported (in R_A units): 10 (Craig and Lupton, 1976); 7.95 ± 0.02 (Kurz and Jenkins, 1981); 8.76 (Allegre et al., 1986/87); 8.2 ± 0.2 (Kurz, 1991); 8.18 ± 0.73 (Hilton et al., 1993a), and 8.11 ± 0.78 (Allegre et al., 1995)-in all cases, the uncertainty is expressed as the estimated SD). For these estimates to be representative of depleted MORB mantle, only samples located distant from obvious plume influences and/or showing no geochemical evidence of plume involvement should be included—a requirement that is difficult to guarantee in all cases. Nevertheless, for compilations made during the last decade, there appears to be good agreement in the various estimates of the mean (depleted) MORB ^{3}He/^{4}He ratio. It is not surprising, therefore, that recent discussions involving MORB-He variations (e.g., Farley and Neroda, 1998; Kurz et al., 1998; Moreira et al., 1999) continue to use 8 ± 1 R_A as the canonical value for MORB mantle. In the present context, the La Palma geothermal fluid value of 9.68 R_A reported by Perez et al. (1996) falls just beyond two SDs from the most recent estimate of the mean value (Allegre et al., 1995). Therefore, we deem it unlikely that the ^{3}He/^{4}He ratio of this geothermal fluid falls within the population that is believed to represent depleted MORB.

Further illustration of the difference between the La Palma fluid ^{3}He/^{4}He ratios and MORB mantle is afforded by Figure 5, in which the La Palma data are compared to regions of the mid-Atlantic Ridge adjacent to the Azores and Canary Island archipelagos. Ignoring the obvious Icelandic plume influence at latitudes north of ~50°, the average ^{3}He/^{4}He ratio for this portion of the midocean ridge system is 8.01 ± 0.68 R_A (n = 43)—in excellent agreement with both the global and North Atlantic means reported by Allegre et al. (op cit.). Excluding samples TR123-5D-3 and -5 located at 32.62°N (9.6 R_A; Kurz et al., 1982b) as other geochemical evidence suggest this location is plume contaminated (see Kingsley and Schilling, 1995), La Palma along with the Azores (11.3 R_A; Moreira et al., 1999) stand conspicuously above the uppermost limit of the MORB range. A lower mantle (plume) influence has been advocated to account for the Azores ^{3}He/^{4}He ratios (Moreira et al., 1999)

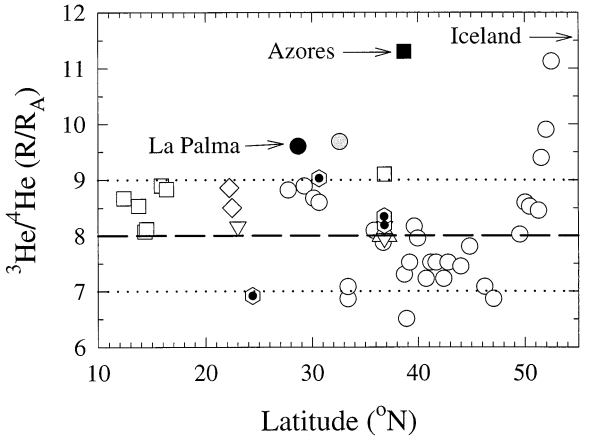

Fig. 5. Comparison of La Palma and the Azores ^{3}He/^{4}He ratios (R/R_A notation)—highest values only are plotted (this work; Moreira et al., 1999)—with adjacent portions of the Mid-Atlantic Ridge. Data sources are: circles (Kurz et al., 1982b); squares (Staudacher et al., 1989); diamonds (Craig and Lupton, 1976); hexagons (Hiyagon et al., 1992); triangles (Marty et al., 1983); inverted triangles (Kurz and Jenkins, 1981). Note the influence of the Icelandic plume at latitudes >50°N and the anomalous MORB sample at 32.6°N (shaded gray) which records a plume influence.

and, although not as prominent, we suggest that La Palma also samples a 'high-^{3}He' plume. It is noteworthy that there is a near continuum in ^{3}He/^{4}He ratios between ~9 and 11.4 R_A at the Azores including values between 9.5 and 9.7 R_A as seen at La Palma. Following the Azores, therefore, we believe that La Palma represents the second locality associated with the eastern Atlantic/European low-velocity anomaly (Hoernle et al., 1995) to record a deep mantle (^{3}He/^{4}He > MORB) connection.

5.3. He Isotope Heterogeneity at La Palma: Geothermal Fluids vs. Phenocryst Helium

The range in ^{3}He/^{4}He ratios at La Palma—also found on other islands in the Canary archipelago (Graham et al., 1996; Vance et al., 1989)—could represent heterogeneities in the Canaries source region (cf. Hoernle and Schmincke, 1993; Widom et al., 1999) caused by mixing phenomena and/or other mantle processes. Before tackling these issues, however, a notable observation for La Palma is that the highest ^{3}He/^{4}He ratios are found in the geothermal fluids of the Taburiente caldera, whereas phenocrysts from the various petrogenetic series apparently sample lower values. In this section, we consider whether any significance should be attached to this observation.

There are two processes that can be envisaged to account for the presence of high ^{3}He/^{4}He ratios in contemporary geothermal fluids at La Palma: 1) incipient mantle melting, involving degassing of He and other volatiles; and 2) leaching or thermal alteration of the lava pile and release of trapped volatiles. Both these possibilities were considered by Hilton et al., (1998a) to account for high ^{3}He/^{4}He ratios in geothermal fluids of northwest Iceland—in that case, the former explanation was favored based upon mass balance arguments and the lack of stability of potential volatile carrier phases in the crust. In the case of La Palma, the contemporary flux of CO_2 released from the active

(southern) part of the island (~590 tons/day; Melian et al., 1997) can be used as a yardstick to consider potential volumes of magma/lava that are needed to supply the measured volatiles fluxes. Assuming that the measured $CO_2/^3He$ ratio for Taburiente caldera (1.7×10^{10}; Table 1) is applicable for the whole island then the present-day ^3He flux for La Palma is ~6.5×10^3 cm^3STP/yr or the equivalent of that supplied by the complete annual degassing of 1.3×10^{-2} km^3 basaltic magma (for a MORB source-type He-content; see Appendix). Alternatively, if leaching of the existing lava pile is the primary means of supplying the ^3He flux then approximately 100 km^3 of crust needs to be processed annually by using a generous estimate of crust containing 20% (by volume) mafic phenocrysts with concentrations of ~10 ncm^3STP^4He/g phenocryst.

Given that the area of La Palma is ~730 km^2, operation of the leaching mechanism would imply that the crust underlying the island would rapidly lose (over the period of decades) its stored He and would be unable to supply the geothermal fluids on a long-term basis. Therefore, we suggest that contemporary degassing of volatiles from magmas stored at different levels within the La Palma lithosphere—as envisaged by Hansteen et al. (see Fig. 6 of Hansteen et al., 1998)—provides the most plausible means of supplying magmatic volatiles to the geothermal system. This mechanism negates having to appeal to the annual hydrothermal processing of significant volumes of the La Palma crust. This degassing mechanism is also consistent with observation of higher $^3He/^4He$ in the fluids relative to the lavas: because magmas stall and degas in the uppermost mantle before eruption, they have the potential to accumulate radiogenic He from surrounding wallrock (we discuss this scenario in Section 5.4). In contrast, geothermal fluids sample the exsolved volatile phase from magmas. This phase would be expected to contain the major proportion of the He inventory of a particular magma batch and, as such, would be much less likely to record modification of its He isotope record. At other localities, e.g., Cerro Negro volcano in Nicaragua, higher $^3He/^4He$ ratios are found in geothermal fluids compared to contemporary OL phenocrysts (Fischer et al., 1999). Therefore, we favor the scenario whereby geothermal fluids provide a minimum estimate of the $^3He/^4He$ ratio of the La Palma mantle, with lavas much more likely to record additions of isotopically anomalous (radiogenic) He en route to the surface by processes related to storage and/or degassing before eruption.

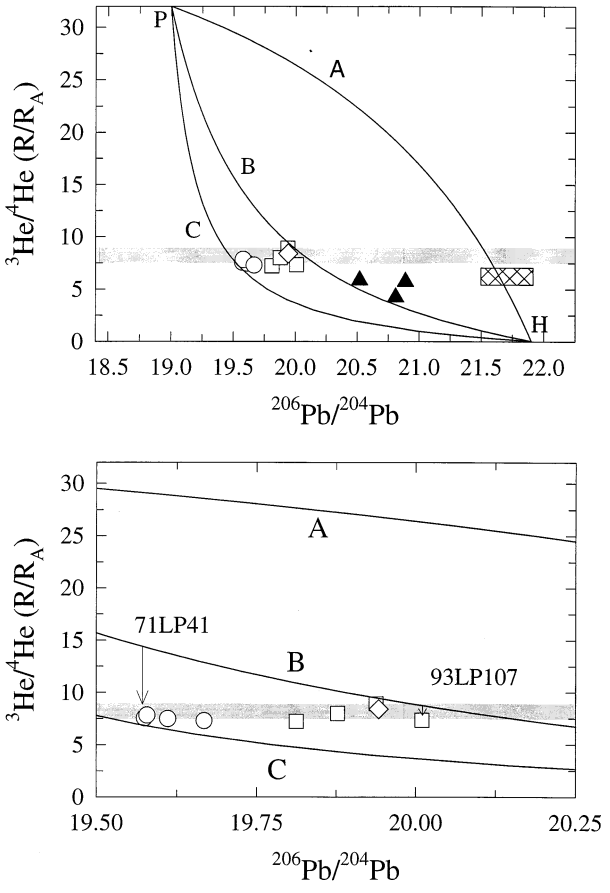

Fig. 6. Plot of He vs. Pb isotope variations for La Palma phenocrysts (Table 1) illustrating binary mixing scenario 1 (Section 5.4.1). Shaded region represents the MORB $^3He/^4He$ ratio. Symbols as in Figure 3. Uppermost plot: Curves represent binary mixing trajectories between a high-^3He plume mantle (P) and a HIMU endmember (H), and are labeled (A) to represent mixing with an undegassed plume and curves B and C to represent depletions of ×12 and ×36, respectively, in the initial plume He content. The crosshatched box represents the range of He–Pb isotopes found at Mangaia (Cook Islands) whereas filled symbols represent St. Helena samples. Lowermost plot: Expanded view of the La Palma dataset emphasizing the two samples characterised by the least (71LP41) and most (93LP107) radiogenic lead isotope compositions of the present sample set. In-growth of radiogenic He to shift these two samples from curve B to curve C would take significant time periods: ~22 and ~6 Myr, respectively (see text).

5.4. He-Pb Isotope Relationships at La Palma: Constraints on Mantle Mixing Hypotheses

The presence of a high-^3He plume component at La Palma effectively rules out the generality of the 'open-system' model used by Hanyu and Kaneoka (1998) to explain $^3He/^4He$ ratios < MORB ($5-8R_A$) observed at other HIMU islands. In this section, therefore, we consider alternative scenarios, also involving mantle mixing ± radiogenic growth of ^4He, guided by the following assumptions and observations: First, three main components only are considered: a) a high $^3He/^4He$ component related to a deep-seated plume source; b) a recycled HIMU component that carries radiogenic He, Pb, and Os; and c) a depleted MORB-mantle source component. Although suggested endmember He–Pb compositions are discussed in the Appendix, we recognize the following caveats: 1) the La Palma case may present a unique evolutionary history so that it may not be related directly to mixing of these common components as observed at other localities (Marcantonio et al., 1995); and 2) additional components might well be present (Widom et al., 1999) which, for the illustrative purposes of the following simple models, we do not include at this stage.

An important constraint we consider in our mixing scenarios is the expectation that melts will rapidly lose their original Os isotopic signature on interaction with mantle of different composition (Hauri and Hart, 1993). The observation that La Palma lavas retain Os isotopic ratios significantly higher than MORB (Marcantonio et al., 1995) thus implies that any mixing of plume and depleted mantle must occur as a solid–solid mix, before melting. The important ramification for He isotope sys-

tematics is that mixing with any MORB component must occur before any possible degassing. Additionally, we consider the possible presence of a radiogenic He component associated with earlier plume melts 'frozen into' the lithosphere beneath the Canary Islands. This scenario could provide considerably greater amounts of radiogenic He—compared to that provided by in-growth with magma chambers, for example—yet avoids the problem of lithospheric contamination lowering the Os isotopic composition as the contaminant is characterised by the same Os isotopic composition as the melt. This process of auto-contamination thereby affects the $^3He/^4He$ ratio only.

5.4.1. Scenario I: Mantle Mixing (Without Involvement of MORB-Mantle)

In this first mantle-mixing hypothesis, we note two lines of argument excluding the involvement of MORB-mantle as a possible endmember:

(a) Entrainment theory indicates that mantle plumes suffer insignificant contamination by MORB-source matrix en route to the surface (Hauri et al., 1994).

(b) As discussed above, preservation of radiogenic (>MORB) Os isotope ratios in the present sample suite and their covariation with lead isotopes indicates that melt movement was sufficiently fast and insulated (e.g., in open channels) to prevent exchange with peridotite of different Os isotope ratio, such as ambient MORB mantle (Hauri and Hart, 1993).

This leaves a high $^3He/^4He$ plume component and a HIMU component as potential endmembers in any mixture with the possibility of a contribution from additional radiogenic ^4He.

In Figure 6, we plot $^3He/^4He$ against $^{206}Pb/^{204}Pb$ ratios for the La Palma samples together with superimposed mixing trajectories between a plume endmember (P), characterised by a high $^3He/^4He$ ratio and intermediate $^{206}Pb/^{204}Pb$, and a HIMU endmember with radiogenic He and radiogenic lead (see Appendix for details). The exact shapes of the mixing lines are determined by the relative (He/Pb) ratios in the endmembers, and we illustrate three cases: first, we mix undegassed P (based on estimates of the closed-system He/Pb ratio of the undepleted mantle) with the HIMU endmember (curve A). We then reduce the [He] in the plume endmember by a factor of 12 and 36 (to trajectories B and C, respectively) so that the mixing trajectories encompass the La Palma data. This seems a more plausible scenario than increasing [He] in the HIMU endmember. There are two pertinent points to note:

(1) The La Palma He–Pb isotope data for the phenocrysts are consistent with a binary mixing scenario between a high $^3He/^4He$ plume and radiogenic HIMU endmembers only if the plume endmember is substantially depleted in He relative to undegassed (lower) mantle (curve A).
(2) The data do not lie along any particular mixing trajectory: rather, they fall between curves B and C.

There are two possibilities to explain these observations: the La Palma plume has experienced variable degrees of degassing so that individual samples define and fall upon their own unique mixing trajectories between curves B and C (Case 1). Alternatively, (Case 2), all samples could have been aligned along a single mixing trajectory (e.g., curve B) with samples bearing the highest $^3He/^4He$ ratios (highest proportion of P) showing proportionally greater isotopic shifts to lower $^3He/^4He$ values by addition of radiogenic He, possibly in the lithospheric mantle.

In the first case (individual mixing trajectories), the prime prerequisite is that the plume component must be characterised by variable (He/Pb) ratios. Shallow-level volatile loss through degassing (cf. Hilton et al., 1997; Poreda et al., 1993) provides a plausible means of producing variable (He/Pb) ratios, irrespective of the ^3He content of the plume (Marty et al., 1996; Marty and Tolstikhin, 1998). Because this variation must be established before mixing with the HIMU endmember, it necessitates siting of the HIMU component in the lithosphere: in this case, this scenario resembles that envisaged for the St. Helena plume beneath the Cameroon line (Halliday et al., 1988). Alternatively, fractionation of the (He/Pb) ratio could occur in the (deeper) mantle (possibly related to a mantle metasomatic event): again, however, formation of a plume with variable (He/Pb) would have to occur before admixture with the HIMU component. Though theoretically possible, a major difficulty with both scenarios is the implication of a fortuitous arrangement of independent mixing trajectories which all must produce a relatively narrow range in $^3He/^4He$ ratios.

If radiogenic He had been added to samples aligned along the same mixing trajectory (Case 2) then samples with the least radiogenic lead (for the present sample set, i.e., the historic lavas) would have experienced the greatest modification in their source $^3He/^4He$ values. For example, the change in He isotope ratio ($\Delta^3He/^4He$) for sample 71LP41 would be 6.66 R_A (it would have a $^3He/^4He$ ratio of 14.33 R_A if it lay on curve B as opposed to a measured value of 7.57 R_A), whereas $\Delta^3He/^4He$ for Tuburiente lava 93LP107 would be only 1.39 R_A. Can magma ageing and/or source enrichment produce the requisite radiogenic He to modify characteristic source $^3He/^4He$ ratios? In the case of sample 71LP41, we calculate its source He concentration to be 8.4×10^{-6} cm^3STP/g based upon it lying on curve B with a mixing proportion of 16.6% of the HIMU endmember. To shift its $^3He/^4He$ ratio by 6.66 R_A, therefore, would require addition of 7.55×10^{-6} cm^3STP^4He/g or a time interval of 22 Myr at a magma U content of 1.6 ppm assuming closed-system conditions. Even for Taburiente sample 93LP107, a similarly large and unrealistic stagnation or mantle ageing time (6.4 Myr) would be required to modify its $^3He/^4He$ ratio. Only an unrealistic tenfold enrichment in U and Th could produce the requisite radiogenic He in periods ~0.6 to 2 Myr—times sufficiently short relative to the volcanic history of La Palma.

We conclude, therefore, that if MORB-mantle is excluded as a potential endmember at La Palma, then mixing between a heterogeneous plume (with variable He/Pb) and a HIMU component sited either in the lithosphere or deeper mantle provides the only plausible explanation for the observed He–Pb isotope systematics. However, this would imply a somewhat fortuitous arrangement of mixing trajectories. The suggestion of Widom et al. (1999) of a further recycled oceanic lithosphere component, similar to but younger than HIMU, would create a range of sources with relatively radiogenic lead isotope ratios and low $^3He/^4He$. This would complicate the mixing model above but not significantly alter the need for a rather

contrived combination of mixing proportions to reproduce the La Palma array.

5.4.2. Scenario II: mantle mixing (With MORB involvement)

Based upon the observation that the La Palma (phenocryst) samples have $^3He/^4He$ ratios close to the MORB ratio (8 ± 1 R_A), we propose an alternative scheme involving mixing between plume and DM mantle ± addition of radiogenic He. In this model, we assume that in chemical terms the plume is a composite body containing a high $^3He/^4He$ component derived from the lower mantle or D[11] and a HIMU component and thus displays both high $^3He/^4He$ (>MORB) and radiogenic Pb. Long-term residence of ancient recycled material in a high-$^3He/^4He$ reservoir would appear to be one plausible means of allowing the plume to acquire such characteristics. Alternatively, both the high and low $^3He/^4He$ ratio endmembers could have evolved separately with their association a result of plume upwelling (see Kellogg et al., 1999). Inclusion of additional components is possible (Widom et al., 1999) but not explicitly modeled here.

In Figure 7, binary mixing trajectories are constructed between plume components B1 and B2 (which differ only in their mantle residence time; see Appendix) and depleted MORB mantle (DMM). The $^3He/^4He$ ratio of the plume component is constrained to lie between the lowest measured value of La Palma (9.6 R_A) and >30 R_A as observed at other plumes (see Farley and Neroda, 1998). However, for $^3He/^4He$ ratios $\gg$ 9.6 R_A, increasingly lower He/Pb ratios in the plume endmember are required to produce the requisite curvature in the mixing trajectories to overlap the La Palma dataset. For example, if the plume had $^3He/^4He = 30$ R_A then lowering of its He/Pb ratio by a factor of ~1000 (from curve A1) is necessary to account for the data by binary mixing (curve A2). As discussed above, plume degassing is a viable means of achieving such low (He/Pb) values: however, degassing (and concomitant melting) would have to occur before mixing with the DMM endmember, a possibility excluded by the radiogenic Os isotope systematics of the La Palma samples. Therefore, we suggest that the composite plume is characterised by a $^3He/^4He$ ratio of ~9.6 R_A negating the requirement of prior plume degassing to produce the requisite mixing trajectories.

In this case, binary mixing provides a plausible explanation for the He–Pb isotope systematics of a number of the La Palma samples (Fig. 7). Mixing between DMM and composite plumes containing either old (B1) or young HIMU (B2) provides a reasonably good fit to the observed data taking analytical uncertainty into account. Furthermore, because the $^3He/^4He$ ratios of the endmembers are close, the mixing trajectories are fairly insensitive to the adopted endmember (He/Pb) values (Appendix). In the case of endmember B1, the La Palma dataset require admixture with between 12 to 19% of the composite plume endmember to account for the observed values: in the case of B2 (plume $^{206}Pb/^{204}Pb = 20.1$), the proportion rises to 39 to 83%. In the former case, there is good agreement with the proportion of HIMU (15 to 30%) estimated from Os–Pb mixing systematics (Marcantonio et al., 1995).

In addition to the binary mixing scenario outlined above, another component is required to account for the lack of detailed correlation between $^3He/^4He$ and $^{206}Pb/^{204}Pb$. Addition

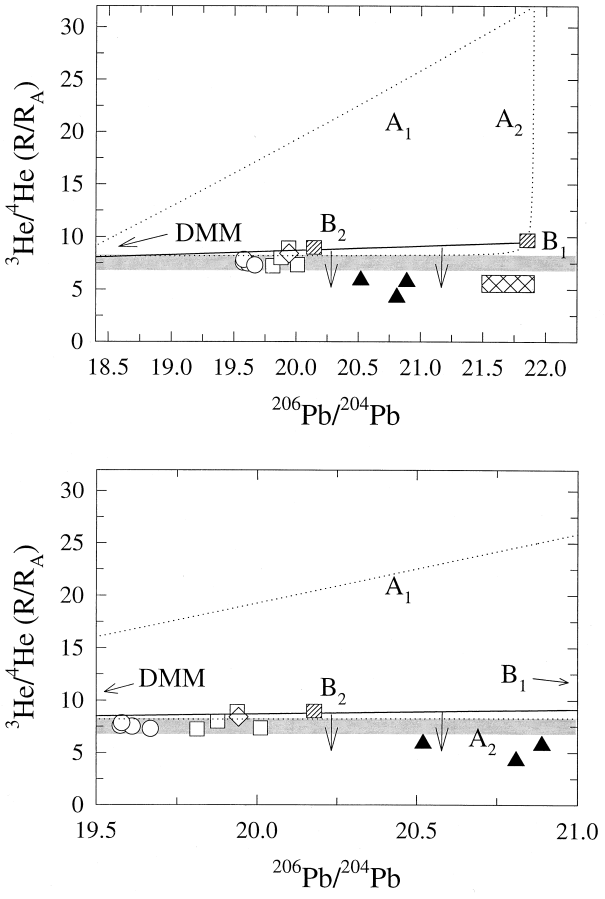

Fig. 7. Plot of He vs. Pb isotope variations for La Palma phenocrysts (Table 1) illustrating binary mixing scenario 2 (Section 5.4.2). Uppermost plot: Lines represent binary mixing trajectories between depleted MORB mantle (DMM) and a high-^3He hotspot endmember (lines labeled A1 and A2) and two HIMU endmembers ($R/R_A = 9.6$) with $^{206}Pb/^{204}Pb = 20.2$ (curve B2) and 21.9 (curve B1) corresponding to young and old HIMU sources, respectively. Curve A2 is depleted in plume He by a factor of 1000 relative to curve A1. The crosshatched box represents the range of He–Pb isotopes found at Mangaia (Cook Islands) and filled symbols are St. Helena samples. Arrows indicate the anticipated trajectories from the mixing curve due to radiogenic He addition (auto-contamination). Lowermost plot: Expanded view of La Palma He–Pb isotope relationships (open symbols) together with St. Helena samples (Graham et al., 1992, filled symbols).

of radiogenic He from melts frozen into the mantle lithosphere may also exert a control on final $^3He/^4He$ ratios at La Palma. For example, isolation of a La Palma melt would produce ~2.6 $\mu cm^3STP/g^4He$ (for U = 5 ppm) in 2 Myr. Being of the same composition, such material could auto-contaminate a DMM-composite plume mixture, have a discernible effect on resultant $^3He/^4He$ ratios and yet not produce concomitant changes to other geochemical tracers. In the case of a 20% admixture of the B1 composite plume endmember to DMM ($R/R_A = 8.3$ and [He] = 17.6 $\mu cm^3STP/g$), then auto-assimilation of 10% material with radiogenic He would give a final $^3He/^4He$ ratio of 7.23 R_A. Note that prior degassing of the DMM-composite plume mixture and/or increasing isolation times of the contaminant can reduce the proportion of assimilated material drastically. Significantly, operation of this mechanism provides a

ready explanation for the difference in $^3He/^4He$ between geothermal fluids and phenocrysts (Section 5.3). We conclude, therefore, that admixture of a composite plume with DMM (± addition of radiogenic He) provides the most plausible means of adding the observed complexity to the He–Pb systematics of La Palma.

5.5. Implications for HIMU Mantle Sources

Finally, we explore the He–Pb systematics of other HIMU islands in the light of the above treatment. He and Pb isotope ratios for St. Helena phenocrysts (analyses obtained on the same samples; Graham et al., 1992) together with the range reported for Mangaia (Hanyu and Kaneoka, 1997; Woodhead, 1996) are plotted in Figures 6 and 7. In the case of the mixing scenario without DMM involvement (Section 5.4.1 and Fig. 6), we note the following points for these two islands:

(1) The St. Helena samples fall very close to mixing curve B indicating that the model of a variably depleted plume mixing with a radiogenic He and Pb HIMU endmember could account for the observed trends. This is not the case for Mangaia which requires a plume undepleted in He as a possible endmember component and/or a more radiogenic Pb plume endmember.
(2) Both St. Helena and Mangaia require a significantly greater proportion of the HIMU endmember relative to La Palma: in the case of St. Helena, the HIMU proportion lies between 46 and 57% for $^{206}Pb/^{204}Pb$ ratios of 20.5 and 20.8 on curve B, respectively. If binary mixing along curve A adequately describes the Mangaia dataset then the proportion of the HIMU component in the mixture increases to ~94% ($^{206}Pb/^{204}Pb = 21.75$).

If this mixing scenario is applicable to these HIMU islands then the high proportion of the HIMU component in both cases may act to obscure the high-^3He plume ratios involved in their petrogenesis. It is unsurprising, then, that the $^3He/^4He$ ratios at St. Helena and Mangaia are not as high as found at La Palma. It is significant that the caveat about fortuitous mixing curves (Section 5.4.1) would apply to the St. Helena case: however, marked enrichment in the He content of the plume mantle, relative to that envisaged for lower mantle (Porcelli and Wasserburg, 1995), would be necessary to account for the Mangaia He–Pb systematics by this mechanism.

In the case involving DMM mixing (Section 5.4.2 and Fig. 7), we note the following possibilities: slightly different proportions of the high-^3He and HIMU components could provide the composite plume endmember (with higher $^{206}Pb/^{204}Pb$ and lower $^3He/^4He$) to account for the St. Helena and Mangaia data. In this case, the composite plume would have to contain a higher proportion of the HIMU component compared to the plume endmember required to account for the La Palma data (Section 5.4.2). Alternatively, if the composite plume is similar to that of La Palma (B1) then St. Helena and Mangaia would require addition of significantly more radiogenic He by autocontamination than required for La Palma.

A crucial aspect of testing these mixing scenarios is finding samples which show variations in their (mixing) proportions of various endmember compositions. An anticipated consequence is that the concentration of He is likely to vary between different samples. For example, samples with a greater proportion of DMM (e.g., St. Helena) would be expected to have a lower final He content than mixtures dominated by the HIMU component (e.g., Mangaia; see Appendix). Although there are a number of factors which determine the final He content of phenocrysts, the source content is likely to be an important contributory one. In this way, we hypothesize that different HIMU island magmas will have different susceptibilities to contamination by addition of radiogenic He. Therefore, more extensive sampling of HIMU islands would seem a pragmatic approach of testing these ideas of binary mixing and addition of radiogenic He. Alternatively, coupling He measurements in HIMU lavas with another volatile tracer (e.g., neon), perhaps more robust in retaining plume signatures (Matsumoto et al., 1997), may also provide constraints on distinguishing and quantifying endmember contributions to HIMU volcanism.

6. CONCLUDING REMARKS

In conclusion, we emphasize the following points:

(1) La Palma is characterized by a range in $^3He/^4He$ values, from 9.6 R_A as observed in present-day geothermal fluids to ratios ~6 to 7 R_A at the lower end of the range normally associated with MORB. La Palma represents the first HIMU ocean island with reported high-^3He (plume) characteristics ($^3He/^4He >$ MORB).
(2) There is no evidence for modification of either geothermal fluid or phenocrysts $^3He/^4He$ ratios: the range in $^3He/^4He$ values, therefore, reflects heterogeneity in the mantle lithosphere source region and is unrelated to processes of magma ageing or crustal contamination.
(3) The He–Pb systematics of La Palma are compatible with two mixing scenarios involving: a) a mantle plume, extensively but variably depleted in its original He content, and a HIMU source; or b) a composite mantle plume, with high $^3He/^4He$ and radiogenic lead, mixing with depleted MORB mantle (DMM). In both cases, addition of radiogenic He (from melts of earlier magmatic pulses frozen into the lithosphere) may act to lower resultant $^3He/^4He$ ratios. We favour scenario (b) above as being a more plausible explanation for the He–Pb isotope relationships of La Palma. We find no need to invoke a radiogenic growth/diffusion model (Hanyu and Kaneoka, 1998) to explain these relationships.
(4) Such mixing models may be applicable to other HIMU islands. However, only $^3He/^4He$ ratios $<$ MORB have been reported for HIMU locations to date: this may result from high proportions (or greater age?) of the HIMU component in any mixture and/or superimposition of radiogenic He masking source $^3He/^4He$ ratios. More extensive sampling of HIMU islands, perhaps coupling He to neon isotope measurements, may provide the basis to test the validity of the suggested binary mixing scenarios.

Acknowledgments—Funds provided by the NERC (UK), the Vrije Universiteit, Amsterdam and the Academic Senate of the University of California supported sample collection. J. Gee and H. Staudigel are thanked for information on locations of geothermal fluids within the Tuburiente caldera. Additionally, we thank L. Findlay for mineral separation, J. Griffith for preparation of Figure 1 and H. Craig for access to instrumentation. Discussion with M. Thirlwall, A. Dickson

and substantive comments by W. White and two anonymous reviewers were very helpful and are much appreciated.

This work was supported by the National Science Foundation Grant EAR96-14347.

REFERENCES

Allegre C. J., Moreira M., and Staudacher T. (1995) $^4He/^3He$ dispersion and mantle convection. *Geophys. Res. Lett.* **22,** 2325–2328.

Allegre C. J., Staudacher T., and Sarda P. (1986/87). Rare gas systematics: Formation of the atmosphere, evolution and structure of the Earth's mantle. *Earth Planet. Sci. Lett.* 81, 127–150.

Ancochea E., Hernan F., Cendrero A., Cantagrel J. M., Fuster J. M., Ibarrola E., and Coello J. (1994) Constructive and destructive episodes in the building of a young oceanic Island, La Palma, Canary Islands, and the genesis of the Caldera de Taburiente. *J. Volcanol. Geotherm. Res.* **60,** 243–262.

Carroll M. R. and Draper D. S. (1994) Noble gases as trace elements in magmatic processes. *Chem. Geol.* **117,** 37–56.

Chauvel C., Hofmann A. W., and Vidal P. (1992) HIMU-EM: The French Polynesian connection. *Earth Planet. Sci. Lett.* **110,** 99–119.

Craig H. and Lupton J. E. (1976) Primordial neon, helium, and hydrogen in oceanic basalts. *Earth Planet. Sci. Lett.* **31,** 369–385.

Elliott T. R. (1991) Element fractionation in the petrogenesis of ocean island basalts. Ph.D. thesis, Open Univ.

Farley K. A., Basu A. R., and Craig H. (1993) He, Sr and Nd isotopic variations in lavas from the Juan–Fernandez archipelago, SE Pacific. *Contrib. Mineral. Petrol.* **115,** 75–87.

Farley K. A. and Craig H. (1992) Mantle plumes and mantle sources. *Science* **258,** 821.

Farley K. A., Natland J. H., and Craig H. (1992) Binary mixing of enriched and undegassed (primitive?) mantle components (He, Sr, Nd, Pb) in Samoan lavas. *Earth Planet. Sci. Lett.* **111,** 183–199.

Farley K. A. and Neroda E. (1998) Noble gases in the Earth's mantle. *Annu. Rev. Earth Planet. Sci.* **26,** 189–218.

Fischer T. P., Roggensack K., Shuster D. L., and Kennedy B. M. (1999) Noble gas isotopic composition of Central American magmas. *EOS Trans. Am. Geophys. Un.* **80,** 1202–1203.

Fisk M. R., Upton B. G. J., Ford C. E., and White W. M. (1988) Geochemical and experimental study of the genesis of magmas of Reunion Island, Indian Ocean. *J. Geophys. Res.* **93,** 4933–4950.

Graham D. W., Christie D. M., Harpp K. S., and Lupton J. E. (1993) Mantle plume helium in submarine basalts from the Galapagos platform. *Science* **262,** 2023–2026.

Graham D. W., Hoernle K. A., Lupton J. E., and Schmincke H.-U. (1996) Helium isotope variations in volcanic rocks from the Canary Islands and Madeira. *Chapman Conference: Shallow Level Processes in Ocean Island Magmatism,* American Geophysical Union (publ.) pp. 13–14.

Graham D. W., Humphris S. E., Jenkins W. J., and Kurz M. D. (1992) Helium isotope geochemistry of some volcanic rocks from Saint-Helena. *Earth Planet. Sci. Lett.* **110,** 121–131.

Halliday A. N., Dickin A. P., Fallick A. E., and Fitton J. G. (1988) Mantle dynamics: A Nd, Sr, Pb and O isotopic study of the Cameroon line volcanic chain. *J. Petrol.* **29,** 181–211.

Hanan B. B. and Graham D. W. (1996) Lead and helium isotope evidence from oceanic basalts for a common deep source of mantle plumes. *Science* **272,** 991–995.

Hansteen T. H., Klugel A., and Schmincke H.-U. (1998) Multi-stage magma ascent beneath the Canary Islands: Evidence from fluid inclusions. *Contrib. Mineral. Petrol.* **132,** 48–64.

Hanyu T. and Kaneoka I. (1997) The uniform and low $^3He/^4He$ ratios of HIMU basalts as evidence for the origin as recycled materials. *Nature* **390,** 273–276.

Hanyu T. and Kaneoka I. (1998) Open system behavior of helium in case of the HIMU source area. *Geophys. Res. Lett.* **25,** 687–690.

Hart S. R., Hauri E. H., Oschmann L. A., and Whitehead J. A. (1992a) Mantle plumes and entrainment—isotopic evidence. *Science* **256,** 517–520.

Hart S. R., Hauri E. H., Oschmann L. A., and Whitehead J. A. (1992b) Mantle plumes and mantle sources—response. *Science* **258,** 821–822.

Hauri E. H. and Hart S. R. (1993) Re–Os isotope systematics of HIMU and EMII oceanic island basalts from the south Pacific Ocean. *Earth Planet. Sci. Lett.* **114,** 353–371.

Hauri E. H., Whitehead J. A., and Hart S. R. (1994) Fluid dynamic and geochemical aspects of entrainment in mantle plumes. *J. Geophys. Res.* **99,** 24275–24300.

Hayes D. E. and Rabinowitz P. D. (1975) Mesozoic magnetic lineations and the magnetic quiet zone off north west Africa. *Earth Planet. Sci. Lett.* **28,** 105–115.

Hilton D. R. (1996) The helium and carbon isotope systematics of a continental geothermal system—results from monitoring studies at Long Valley caldera (California, USA). *Chem. Geol.* **127,** 269–295.

Hilton D. R., Barling J., and Wheller G. E. (1995) Effect of shallow-level contamination on the helium isotope systematics of ocean-island lavas. *Nature* **373,** 330–333.

Hilton D. R., Gronvold K., Macpherson C. G., and Castillo P. R. (1999) Extreme $^3He/^4He$ ratios in northwest Iceland: Constraining the common component in mantle plumes. *Earth Planet. Sci. Lett.* **173,** 53–60.

Hilton D. R., Gronvold K., O'Nions R. K., and Oxburgh E. R. (1990) Regional distribution of ^3He anomalies in the Icelandic crust. *Chem. Geol.* **88,** 53–67.

Hilton D. R., Gronvold K., Sveinbjornsdottir A., and Hammerschmidt K. (1998a) Helium isotope evidence for off-axis degassing of the Icelandic hotspot. *Chem. Geol.* **149,** 173–187.

Hilton D. R., Hammerschmidt K., Loock G., and Friedrichsen H. (1993a) Helium and argon isotope systematics of the central Lau Basin and Valu Fa ridge: Evidence of crust–mantle interactions in a back-arc basin. *Geochim. Cosmochim. Acta* **57,** 2819–2841.

Hilton D. R., Hammerschmidt K., Teufel S., and Friedrichsen H. (1993b) Helium isotope characteristics of Andean geothermal fluids and lavas. *Earth Planet. Sci. Lett.* **120,** 265–282.

Hilton D. R., McMurtry G. M., and Goff F. (1998b) Large variations in vent fluid $CO_2/^3He$ ratios signal rapid changes in magma chemistry at Loihi seamount, Hawaii. *Nature* **396,** 359–362.

Hilton D. R., McMurtry G. M., and Kreulen R. (1997) Evidence for extensive degassing of the Hawaiian mantle plume from helium-carbon relationships at Kilauea volcano. *Geophys. Res. Lett.* **24,** 3065–3068.

Hiyagon H., Ozima M., Marty B., Zashu S., and Sakai H. (1992) Noble gases in submarine glasses from mid-oceanic ridges and Loihi Seamount—constraints on the early history of the Earth. *Geochim. Cosmochim. Acta* **56,** 1301–1316.

Hoernle K. and Schmincke H.-U. (1993) The role of partial melting in the 15-Ma geochemical evolution of Gran Canaria: A blob model for the Canary hotspot. *J. Petrol.* **34,** 599–626.

Hoernle K., Zhang Y. S., and Graham D. (1995) Seismic and geochemical evidence for large-scale mantle upwelling beneath the eastern Atlantic and western and central Europe. *Nature* **374,** 34–39.

IAEA. (1992) *Statistical Treatment of Data on Environmental Isotopes in Precipitation.* IAEA.

Jochum K. P., Hofmann A. W., Ito E., Seufert H. M., and White W. M. (1983) K, U and Th in mid-ocean ridge glasses and heat production, K/U and K/Rb in the mantle. *Nature* **306,** 431–436.

Kellogg L. H., Hager B. H., and van der Hilst R. D. (1999) Compositional stratification in the deep mantle. *Science* **283,** 1881–1884.

Kingsley R. H. and Schilling J. G. (1995) Carbon in Mid-Atlantic Ridge basalt glasses from 28°N to 63°N: Evidence for a carbon-enriched Azores mantle plume. *Earth Planet. Sci. Lett.* **129,** 31–53.

Klugel A. (1998) Reactions between mantle xenoliths and host magma beneath La Palma (Canary Islands): Constraints on magma ascent rates and crustal reservoirs. *Contrib. Mineral. Petrol.* **131,** 237–257.

Klugel A., Hansteen T. H., and Schmincke H.-U. (1997) Rates of magma ascent and depths of magma reservoirs beneath La Palma (Canary Islands). *Terra Nova* **9,** 117–121.

Kurz M. D. (1991) Noble gas isotopes in oceanic basalts: Controversial constraints on mantle models. In *Applications of Radiogenic Isotope Systems to Problems in Geology* (ed. L. Heaman and J. N. Ludden), pp. 259–286. Publ. Mineral. Assoc. (Canada).

Kurz M. D. and Jenkins W. J. (1981) The distribution of helium in oceanic basalt glasses. *Earth Planet. Sci. Lett.* **53,** 41–54.

Kurz M. D., Jenkins W. J., and Hart S. R. (1982a) Helium isotope systematics of ocean islands and mantle heterogeneity. *Nature* **297,** 43–47.

Kurz M. D., Jenkins W. J., Hart S. R., and Clague D. (1983) Helium isotopic variations in Loihi Seamount and the island of Hawaii. *Earth Planet. Sci. Lett.* **66,** 388–406.
Kurz M. D., Jenkins W. J., Schilling J. G., and Hart S. R. (1982b) Helium isotopic variations in the mantle beneath the central north Atlantic Ocean. *Earth Planet. Sci. Lett.* **58,** 1–14.
Kurz M. D., LeRoex A. P., and Dick H. J. B. (1998) Isotope geochemistry of the oceanic mantle near the Bouvet triple junction. *Geochim. Cosmochim. Acta* **62,** 841–852.
Macpherson C. G., Hilton D. R., Sinton J. M., Poreda R. J., and Craig H. (1998) High $^3He/^4He$ ratios in the Manus backarc basin: Implications for mantle mixing and the origin of plumes in the western Pacific Ocean. *Geology* **26,** 1007–1010.
Marcantonio F., Zindler A., Elliott T., and Staudigel H. (1995) Os isotope systematics of La Palma, Canary Islands—evidence for recycled crust in the mantle source of HIMU ocean islands. *Earth Planet. Sci. Lett.* **133,** 397–410.
Marty B. and Jambon A. (1987) $C/^3He$ in volatile fluxes from the solid Earth: Implication for carbon geodynamics. *Earth Planet. Sci. Lett.* **83,** 16–26.
Marty B., Pik R., and Gezahegn Y. (1996) Helium isotopic variations in Ethiopian plume lavas—nature of magmatic sources and limit on lower mantle contribution. *Earth Planet. Sci. Lett.* **144,** 223–237.
Marty B. and Tolstikhin I. N. (1998) CO_2 fluxes from mid ocean ridges arcs and plumes. *Chem. Geol.* **145,** 233–248.
Marty B., Trull T., Lussiez P., Basile I., and Tanguy J. C. (1994) He, Ar, O, Sr and Nd isotope constraints on the origin and evolution of Mount Etna magmatism. *Earth Planet. Sci. Lett.* **126,** 23–39.
Marty B., Zashu S., and Ozima M. (1983) Two noble gas components in a mid-Atlantic ridge basalt. *Nature* **302,** 238–240.
Matsumoto T., Honda M., McDougall I., Yatsevich I., and O'Reilly S. Y. (1997) Plume-like neon in a metasomatic apatite from the Australian lithospheric mantle. *Nature* **388,** 162–164.
Melian G. et al. (1997) Diffuse emission of carbon dioxide from the active volcanic zone of La Palma, Canary Islands. *EOS Trans. Am. Geophys. Soc.* **78,** 779.
Moreira M., Doucelance R., Kurz M. D., Dupre B., and Allegre C. J. (1999) Helium and lead isotope geochemistry of the Azores archipelago. *Earth Planet. Sci. Lett.* **169,** 189–205.
Morrison P. and Pine J. (1955) Radiogenic origin of the helium isotopes in rock. *Annu. NY Acad. Sci.* **62,** 69–92.
O'Nions R. K. and Tolstikhin I. N. (1996) Limits on the mass flux between lower and upper mantle and stability of layering. *Earth Planet. Sci. Lett.* **139,** 213–222.
Perez N. M., Nakai S., Wakita H., Hernandez P. A., and Salazar J. M. (1996) Helium-3 emission in and around Teide volcano, Tenerife, Canary Islands, Spain. *Geophys. Res. Lett.* **23,** 3531–3534.
Porcelli D. and Wasserburg G. J. (1995) Mass Transfer of helium, neon, argon, and xenon through a steady-state upper mantle. *Geochim. Cosmochim. Acta* **59,** 4921–4937.
Poreda R. J., Craig H., Arnorsson S., and Welhan J. A. (1992) Helium isotopes in Icelandic geothermal systems 1. He-3, gas chemistry, and C-13 relations. *Geochim. Cosmochim. Acta* **56,** 4221–4228.
Poreda R. J., Schilling J. G., and Craig H. (1993) Helium isotope ratios in Easter microplate basalts. *Earth Planet. Sci. Lett.* **119,** 319–329.
Rison W. and Craig H. (1983) Helium isotopes and mantle volatiles in Loihi Seamount and Hawaiian Islands basalts and xenoliths. *Earth Planet. Sci. Lett.* **66,** 407–426.
Sarda P. and Graham D. (1990) Mid-ocean ridge popping rocks—implications for degassing at ridge crests. *Earth Planet. Sci. Lett.* **97,** 268–289.
Staudacher T., Sarda P., Richardson S. H., Allegre C. J., Sagna I., and Dmitriev L. V. (1989) Noble gases in basalt glasses from a mid-Atlantic ridge topographic high at 14°N—geodynamic consequences. *Earth Planet. Sci. Lett.* **96,** 119–133.
Staudigel H., Feraud G., and Giannerini G. (1986) The history of intrusive activity on the island of La Palma (Canary Islands). *J. Volcanol. Geothermal. Res.* **27,** 299–322.
Staudigel H. and Schmincke H.-U. (1984) The Pliocene seamount series of La Palma/Canary Islands. *J. Geophys. Res.* **89,** 11195–11215.
Sun S.-S. and McDonough W. F. (1989) Chem. and isotopic systematics of oceanic basalts: implications for mantle composition and processes. In *Magmatism in the ocean basins* (ed. A. D. Saunders and M. J. Norry), Geological Society Special Publ. 11042, pp. 313–345.
Theodorsson P. (1967) Natural tritium in groundwater studies. *Isotopes Hydrol.* Proc. Symp. Isotopes in Hydrology, IAEA (Vienna) 371–380.
Thirlwall M. F. (1997) Pb isotopic and elemental evidence for OIB derivation from young HIMU mantle. *Chem. Geol.* **139,** 51–74.
Trull T., Nadeau S., Pineau F., Polve M., and Javoy M. (1993) C-He systematics in hotspot xenoliths—implications for mantle carbon contents and carbon recycling. *Earth Planet. Sci. Lett.* **118,** 43–64.
Trull T. W. and Kurz M. D. (1993) Experimental measurements of ^3He and ^4He mobility in olivine and clinopyroxene at magmatic temperatures. *Geochim. Cosmochim. Acta* **57,** 1313–1324.
Vance D., Stone J. O. H., and O'Nions R. K. (1989) He, Sr and Nd isotopes in xenoliths from Hawaii and other oceanic islands. *Earth Planet. Sci. Lett.* **96,** 147–160.
Weaver B. L. (1991) Trace element evidence for the origin of ocean–island basalts. *Geology* **19,** 123–126.
Widom E., Hoernle K. A., Shirey S. B., and Schmincke H.-U. (1999) Os isotope systematics in the Canary Islands and Madeira: Lithospheric contamination and mantle plume signatures. *J. Petrol.* **40,** 279–296.
Woodhead J. D. (1996) Extreme HIMU in an oceanic setting—the geochemistry of Mangaia Island (Polynesia), and temporal evolution of the Cook–Austral hotspot. *J. Volcanol. Geotherm. Res.* **72,** 1–19.
Zindler A. and Hart S. (1986) Helium: problematic primordial signals. *Earth Planet. Sci. Lett.* **79,** 1–8.

APPENDIX

He–Pb Endmember Isotope and Abundance Characteristics

Table 2 summarizes the He and lead endmember isotope and abundance characteristics used in constructing the binary mixing trajectories in Figures 6 and 7. In scenario 1 (Section 5.4.1 and Fig. 6) the He isotope characteristics of P is taken as 32 R_A, as approximated by the highest ratios measured for Loihi Seamount (Kurz et al., 1983). This is necessary to account for the geothermal fluid value of 9.6 R_A measured for Taburiente caldera which must contain a high-^3He component. We assume that the HIMU source is devoid of primordial ^3He and is characterized solely by radiogenic He produced by in situ decay ($\sim 0.05 R_A$; Morrison and Pine, 1955). The plume lead isotopic composition ($^{206}Pb/^{204}Pb$) is taken somewhat arbitrarily as 19 in order to be less radiogenic than the range observed at La Palma. Note, however, that this value overlaps with suggested values of the high $^3He/^4He$ component in plumes—FOZO (18.5–19.5) (Hart et al., 1992a) and PHEM (18.5–19) (Farley et al., 1992), and is only slightly below the value suggested for C (19.2–19.8; Hanan and Graham, 1996). The value adopted for HIMU $^{206}Pb/^{204}Pb$ (21.9) is based upon the most radiogenic $^{206}Pb/^{204}Pb$ ratio reported to date, (Mangaia, Woodhead, 1996).

The He abundance of P is taken as 56×10^{-6} cm^3STP/g, based on mass balance arguments of lower mantle He (Porcelli and Wasserburg, 1995), whereas the lead concentration of 0.185 ppm is based upon the

Table 2. Endmember He and lead compositions used to construct binary mixing trajectories in Figures 6 and 7.

Endmember	$^3He/^4He$ (R/R_A)	[He] $\mu cm^3STP/g$	$\frac{^{206}Pb}{^{204}Pb}$	[Pb] ppm
P(A)	32	56	19.0	0.185
P(B)	32	4.5	19.0	0.185
P(C)	32	1.5	19.0	0.185
HIMU	0.05	28	21.9	0.23
A1	32	56	21.9	0.23
A2	32	0.056	21.9	0.23
B1	9.6	14	21.9	0.23
B2	9.6	28	20.2	0.23
DMM	8.0	15	18.24	0.058

primitive mantle estimate (Sun and McDonough, 1989). Lead in the HIMU endmember is taken as 0.23 ppm (Chauvel et al., 1992). This latter value is constant irrespective of the timing of an ancient subduction event (2 or 1 Ga). The U concentration of HIMU-source material is similar to present-day MORB (0.066 ppm; Chauvel et al., 1992) implying that loss of Pb during subduction zone processing is the principal control on the generation of the HIMU ratio. Closed-system in-growth of radiogenic He over 2 Gyr, therefore, would produce $\sim 2.8 \times 10^{-5}$ cm^3STP/g assuming a Th/U ratio of 3.3 (Jochum et al., 1983). This value is adopted for the He content of the HIMU endmember. Plume degassing prior to mixing with the HIMU component would act to reduce [He] in the high-^{3}He endmember, and the mixing trajectories B and C reflect a $\times 12$ and $\times 36$ depletion, respectively, with respect to undegassed P (curve A).

In Figure 7 (Section 5.4.2), we assume that the plume endmember is characterized by a $^3He/^4He$ ratio of 9.6 R_A, which is equal to the highest value measured at La Palma (Table 1), whereas the He isotope characteristics of DMM is taken as 8.0 R_A (Hilton et al., 1993a). The DMM lead endmember is taken as the average of present-day Pacific MORB ($^{206}Pb/^{204}Pb = 18.24$; Chauvel et al., 1992) whereas two values are adopted for HIMU $^{206}Pb/^{204}Pb$. In the first case, the adopted value of 21.9 is based upon the radiogenic $^{206}Pb/^{204}Pb$ ratio of Mangaia. In the second case, we use a value of 20.2 or only slightly more radiogenic than the La Palma range. This ratio implies that the La Palma HIMU endmember is of the 'Young HIMU' variety (e.g. Thirlwall, 1997) also approximated by a two-stage evolution history: however, in this case, involving relatively recent subduction ($\sim$1 Ga ago) of oceanic crust with a high $^{238}U/^{204}Pb$ ratio ($\mu = 22$) as opposed to more ancient subduction ($\sim$2 Ga) necessary to account for the Mangaia lead isotope systematics (Chauvel et al., 1992).

The He abundance of DMM is taken as 15×10^{-6} cm^3STP/g by using the He abundance characteristics of the mid-Atlantic popping rock (Staudacher et al., 1989) and the mass balance arguments of Sarda and Graham (Sarda and Graham, 1990). The lead concentration of DMM is 0.058 ppm (Chauvel et al., 1992). Closed-system in-growth of radiogenic He over 1 Gyr, would produce $\sim 1.4 \times 10^{-5}$ cm^3STP/g, which is one half as much He as in the old HIMU case above. Mixing between this endmember and DMM follows line A1 in Figure 7. Prior plume degassing (e.g. Hilton et al., 1997; Poreda et al., 1993) would act to reduce [He] in the high-^{3}He and both HIMU endmembers, and the mixing trajectories (A2) illustrates the effect of a 1000-fold reduction in the hotspot [He].

Finally, we note that mixing trajectories on the same $^3He/^4He$ vs. $^{206}Pb/^{204}Pb$ plot by Hanyu and Kaneoka (1998), assuming the same endmember isotopic compositions, are concave upwards because their value for DMM [He] ($1.1–3.4 \times 10^{-6}$ cm^3STP/g, fully 1 order of magnitude less than is adopted here) is so low. This range is based upon whole-mantle model estimates (O'Nions and Tolstikhin, 1996; Porcelli and Wasserburg, 1995). However, their HIMU [He] value (1.7×10^{-5} cm^3STP/g), based on scaling excess in HIMU $^{206}Pb/^{204}Pb$, $^{207}Pb/^{204}Pb$ and $^{208}Pb/^{204}Pb$ relative to present-day MORB using assumed HIMU Pb isotope ratios is much closer to our value. It is crucial to note that the choice of (endmember) mantle He contents has a defining influence on the mixing trajectories in He–Pb isotope space, and on the type of mixing behavior envisaged.